

NJC

Accepted Manuscript



This is an *Accepted Manuscript*, which has been through the Royal Society of Chemistry peer review process and has been accepted for publication.

Accepted Manuscripts are published online shortly after acceptance, before technical editing, formatting and proof reading. Using this free service, authors can make their results available to the community, in citable form, before we publish the edited article. We will replace this *Accepted Manuscript* with the edited and formatted *Advance Article* as soon as it is available.

You can find more information about *Accepted Manuscripts* in the [Information for Authors](#).

Please note that technical editing may introduce minor changes to the text and/or graphics, which may alter content. The journal's standard [Terms & Conditions](#) and the [Ethical guidelines](#) still apply. In no event shall the Royal Society of Chemistry be held responsible for any errors or omissions in this *Accepted Manuscript* or any consequences arising from the use of any information it contains.



Journal Name

ARTICLE

Heterogeneous Catalysis of Water Oxidation Supported by a Novel Metallamacrocyclic

Wei-Bin Yu*, Qing-Ya He, Hua-Tian Shi, and Xianwen Wei

+++++Received
00th January 20xx,
Accepted 00th January 20xx

DOI: 10.1039/x0xx00000x

www.rsc.org/

The rational design and syntheses of the newly tetranuclear macrocycles $[\text{Cp}^*\text{Ir(L)}]_4(\text{OTf})_4$ (**1**) and $[\text{Cp}^*\text{Rh(L)}]_4(\text{OTf})_4$ (**2**) were successfully achieved through the reaction of pyridyl-substituted ligand 3-(pyridin-3-ylazo)-naphthalen-2-ol (HL) with $[\text{Cp}^*\text{M}(\mu\text{-Cl})\text{Cl}]_2$ (M = Ir, Rh), which was preliminarily treated by AgOTf. The novel macrocycles **1** and **2** were structurally characterized by EA, IR and NMR to confirm their elementary components and frameworks. Further classification of their molecular structures via single crystal X-ray analysis was strongly proved their tetranuclear macrocyclic structures. The systematic investigation of electronic property of complex **1** via cyclic voltammograms (CVs), clearly suggested that it had great potential application as catalysts for water oxidation. Thus the use of complex **1** as a catalyst for water oxidation was performed in the presence of sacrificial chemical oxidation, and afforded a good efficiency reached up to 2.47 min^{-1} .

Introduction

With the development of supramolecular chemistry,¹ coordination-driven self-assembly, which is a classical and traditional procedure for coordination chemistry, has gradually grown up to be a controllable and highly efficient methodology for the construction of supramolecular organometallic architectures, including two-dimensional and three-dimensional complexes with well-defined shapes and sizes.² The energy range of the moderate bonding, which is directly formed by coordination-driven self-assembly, is 15–50 kcal/mol, resulting in considerable stabilities of these supramolecular coordination complexes. The predictable structures of the coordination complexes are primarily directed by their orientational features in coordination chemistry, giving rise to a great number of discrete supramolecular organometallic polygons such as squares, rhomboids, triangles and hexagons, some of which have been explored a wide range of applications in the areas of catalysis, sensors, supramolecular devices, etc.^{3,4} Hierarchical self-assembly, which is a newly procedure of synthesizing metallacyclic skeletons, can be easily introduced into the design of the well-

defined core structures for the metallacycles.⁵ Meanwhile, the hierarchical self-assembly can also provide a approach of forming mono-component metallacycles, which have exhibited a potential properties of host-guest chemistry, transformation of structure, electrochemistry and so on.⁶

In light of principle of coordination-driven self-assembly, the use of metal centers and organic linkers as building blocks has played a key role in the buildup of metallamacrocyclic structures. Half-sandwich iridium and rhodium motifs have been considerable used as corners in the construction of discrete macrocycles, due to their relative stability and inertness toward substitution reactions, and advantageous physical properties, like solubilities, thermal stabilities, and others needed for flexibility in fine-tuning processes.⁶ The half-sandwich Cp^*M (M = Ir, Rh) units as corners in various framework geometries are of a basic three-legged piano-stool shape, where the piano-stool-leg can be variably connected with N-, O-, S-, or P-donor ligands. In this work and in an effort to develop new metallamacrocyclic structures, a pyridyl-substituted ligand based on azo-compound is skillfully designed as relatively rigid bridges with a bridging angle of 90° between the naphthol group and the $\text{N}_{\text{pyridyl}}$ connecting atoms. The ligand containing both binding sites; a monodentate and a chelating unit as shown in Scheme 1, is herein recognized as particularly useful linkages in the construction of large ring arrangements.⁶

On the other hand, the use of half-sandwich iridium complexes as the water oxidation catalysts (WOCs), which have currently become a promising strategy for meeting growing energy demands, has rapidly emerged recently.⁷ Compared to other compounds,^{8–23} they based on organometallic complexes have been one of the most attractive new fields in the realm of WOCs, due to their own superiority on improving catalytic efficiency.^{6a,b} Otherwise, the

a Dr. W. -B. Yu, Q. -Y. He, H. -T. Shi, and Prof. Dr. X. Wei

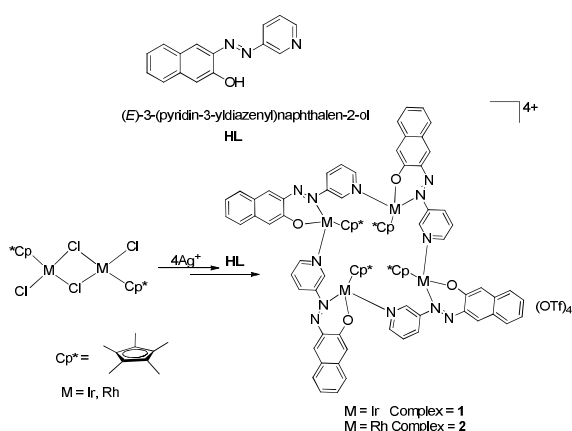
Analysis and Testing Central Facility, School of Chemistry and Chemical Engineering,
Anhui University of Technology,
Maanshan 243002, P.R.China.
Fax: (+) +86 555 2311087;
E-mail: yuweibin@ahut.edu.cn.

Electronic Supplementary Information (ESI) for this article is given via a link at the end of the document.

evolutionary bottleneck of the WOCs is used as sustainable source of electrons and maximizing overall efficiency.²⁴ The employment of complexes constructed by half-sandwich motifs as catalysts of water oxidation is a highly effective method for meeting the requirements.^{6a,b}

A series of WOCs based on half-sandwich iridium fragments, which exhibit a high turnover frequency, have been continuously explored.⁶ Among these compounds, the discovery of use of various azo-ligand to construct the WOCs and organometallic macrocycles is significant for us to explore several complexes. Herein, a newly azo-compound is employed as an organic linker to construct novel metallamacrocycles based on half-sandwich Ir/Rh motifs (Scheme 1), and we further detailedly investigate their effects on water oxidation catalysts.

Results and Discussion



Scheme 1. The syntheses of metallamacrocycles **1** and **2**.

Characterization and Structures

The complementary building blocks must be structurally rigid with predefined bite angles, which is one vital structural requirement for the construction of supramolecular architectures in terms of the principles of coordination-driven assembly. Taking into this consideration, the organic ligands utilized as donor building blocks must have two or more binding sites possessing angular orientations ranging from 0° to 180°. In addition, metal-center subunits employed as acceptors are at a fixed angle relative to one another for binding incoming ligands. In other words, the shape of a target architecture is guided by the symmetry and number of binding sites within each precursor unit. A molecular square, for an example, can be accessed in different ways: the combination of four ditopic 90° angular units and four 180° linear units or the 2:2 assembly of two different 90° angular units.²⁵

According to above mentioned, the final size and shape of a discrete metallacycle is dominantly depended on the angle of the selected building blocks.²⁵ Simply put, a discrete tetragonal

metallacycle can be combined by four building blocks with coordination angle of 90° and four corners with symmetrical angle of 180°. In this work, a new functionalized azo-compound (3-pyridyl donor HL) with coordinating vector of 90° (Chart 1) and three-leg-piano-stool archetype of half-sandwich Ir/Rh fragments (Cp*Ir/Rh) acceptors were employed to construct tetranuclear metallacycles.

In this context, tetranuclear metallacycles [(Cp*Ir)(L)]₄(OTf)₄ **1** (Fig.s2 in ESI) and [(Cp*Rh)(L)]₄(OTf)₄ **2** (Fig.s3 in ESI) with distorted tetragonal metal-based geometries (Scheme 1) were controllable synthesized from the two-step reactions of (Cp*MCl₂)₂ (M = Ir, Rh) with initial activation by AgOTf to create labile coordination sites and sequentially via reaction with the pyridyl-substituted azo-compound ligands (HL), which was synthesized according to the previous work in high yield (80%).²⁶ As Scheme 1 shown, when (Cp*MCl₂)₂ (M = Ir, Rh) was treated with four equivalents of AgOTf followed by separation of the AgCl precipitate, the subsequent reactions with the ligands of type HL afforded the desired crystalline compounds **1** (yield: 65%) and **2** (yield: 71%). Thermal gravimetric analysis (TGA) of **1** and **2** revealed no weight loss when heated over 350 °C (see ESI), indicating that both of products were air and also thermally stable. The IR spectra showed a strong band at approximately 1640 cm⁻¹ for **1** and 1635 cm⁻¹ for **2**, owing to the ν_{C=O} stretching of the bridging azo-compound ligands.

Multinuclear NMR (¹H, ¹³C and ¹⁹F) analysis of these complexes revealed the formation of discrete metallacycles **1** and **2** with highly symmetric structures. For instance, both the ¹⁹F{¹H} NMR spectra of **1** and **2** displayed a sharp singlet (-77.777 ppm for **1** (Fig.s7 in ESI) and -77.774 ppm for **2**, respectively (Fig.s10 in ESI)), primarily proving that identical circumstance of fluorine atom from OTf anions. Highly recognizable feature of the ¹H NMR spectrum unambiguously exhibited a sharp singlet for Cp* group (1.60 ppm for **1** and 1.3 ppm for **2**, respectively) and downfield shift for organic ligand, clearly supporting that highly symmetrical geometry of their molecular structures. Complexes **1** and **2** were soluble in common polar organic solvents, such as CH₂Cl₂, DMSO and MeOH.

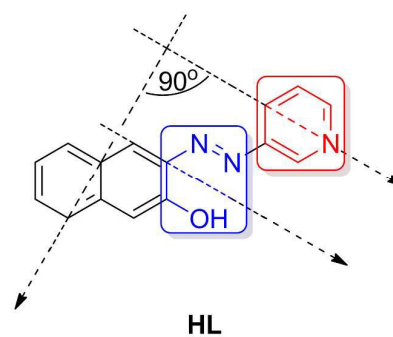


Chart 1. Coordination vectors of HL.

Detailed structural information of complexes **1-2** came from single-crystal X-ray diffraction analyses. As a result, the molecular structures of them turn out to be very similar, compound **1** selected is predominantly discussed. Ball-stick mode drawings of **1** and **2** is

shown in Fig. 1a. According to the figure depicted, a novel tetranuclear metallacycle is unambiguously exhibited. The four η^5 -Cp*M motifs are bridged by four L ligands. Each metal center is occupied by one O_{phenyl} atom and two N atoms (one is from azo group and the other comes from pyridyl group, respectively), forming the classic three-legged-piano-stool architecture. In a simplified view, the geometry of the tetranuclear metallacycle can be described as a distorted rhomboid (Fig.1b). The Ir atoms is located at the four vertices of the rhomboid with adjacent edges of 7.15 Å and 6.04 Å, and the four edges are occupied by the bridging ligands to result in metal-metal-metal angles of 105.4° (Ir2-Ir1-Ir2'), 74.6° (Ir1-Ir2-Ir1'), 98.7° (Ir2-Ir1'-Ir2') and 81.0° (Ir1'-Ir2'-Ir1). Furthermore, the top and bottom faces is slightly opening, in whose distances between naphthol group and pyridyl group are 3.46 Å, so it can't provide a enough spacer for capturing the counterions (OTf⁻).

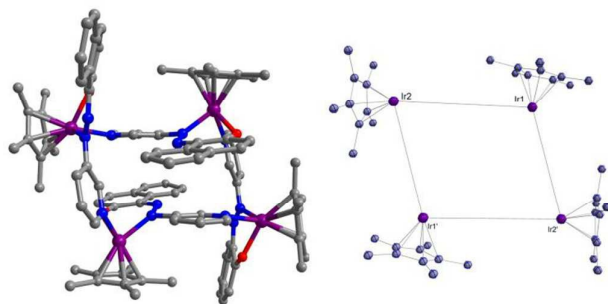


Fig. 1. Left) The structure of metallamacrocycles **1** and **2** in ball-stick mode; Right) Compound **1** can be described as a distorted tetragonal rhomboid, in which the metals occupy the vertices, and the pyridine-substituted azo-compound ligands link these vertices along the drawn red lines (the graphical sketch is based on the true crystal structure of **1**); OTf⁻, solvent molecules and H atoms are omitted for clarify. Dark red, Ir/Rh; Red, O; Blue, N; Gray, C.

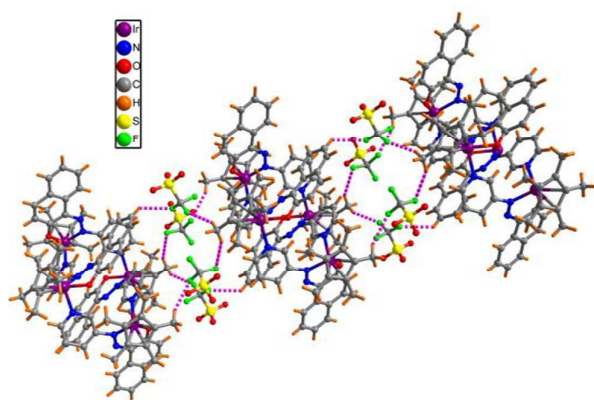


Fig. 2. Stacking of the molecules in crystals of **1** viewed along the *b*-axis by H-bonds.

On the other hand, hydrogen bands in organometallic supramolecular structures have considerably extended the scope

for tuning within this class of compounds. The C-H...F hydrogen band (range of distances is 2.355-2.872Å) is also exhibited in Fig. 2. This type of hydrogen bonding is expected to be weak, however, the force is apparently large enough to bridge two adjacent macrocycles to further create channel architectures along the crystallographic *b*-axis.

Photo and Electronic Properties

Spectrochemical experimental were performed on organometallic macrocycles **1** and **2** to evaluate the effects between metal cation and coordination mode on the electronic structures. As exemplified in Fig. 3, the electronic spectra of the both macrocycles display a broad absorption band in the visible region (530 nm for **1** and 512 nm for **2**, respectively) as a common feature of azo motifs. In contrast, the λ_{max} values of a π - π^* transition band ascribing to the azo moiety in the *trans* form of this ligand is about at 450 nm, suggesting that complexes **1** and **2** give strong bands between L and metal in this region.⁶ On the other hand, the features of spectra for closed complexes **1** and **2** are significantly different from the separation n - π^* bands, which display double low-intensity n - π^* bands in the 300-400 nm region (327 nm for **1** and 337 nm for **2**, respectively).

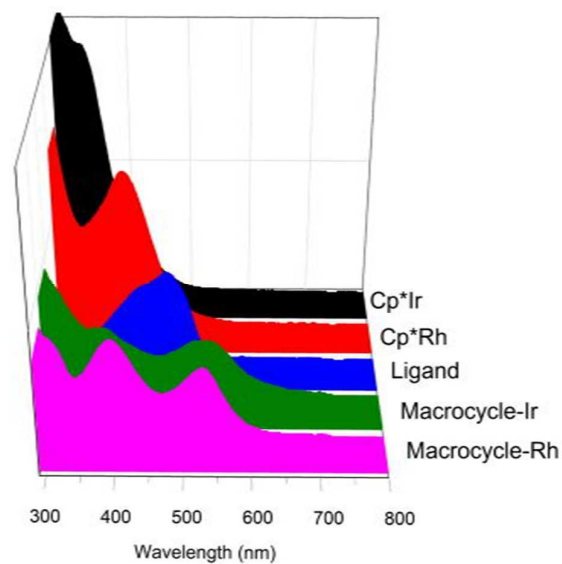


Fig. 3. UV-vis spectra of macrocycles **1**, **2** and related to compounds in methanol.

The good solubility of **1** in water allowed us to examine electronic properties, confirming whether it can drive water oxidation or not in the presence of sacrificial chemical oxidants. Cyclic voltammograms (CVs) were carried out on complex **1** in water solution at room temperature and collected at various pH values (ranges from 4.0 to 11.0) (Fig. 4). The conditions, which supported CVs performing on the complex, were set as PBS (Phosphate Buffered Saline) solution (the concentration was 0.03 mM) utilized as assistant electrolyte with scan rate of 50 mV/s.

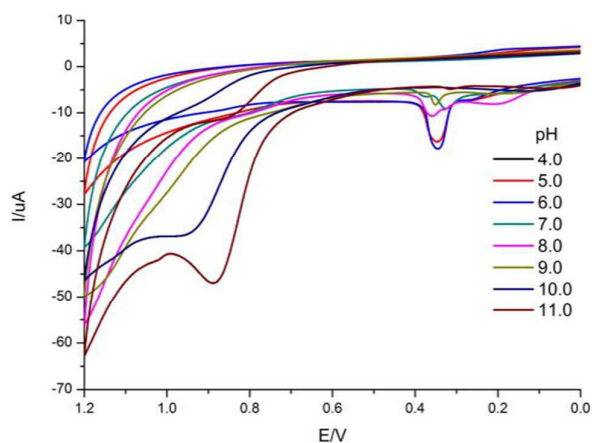


Fig. 4. pH-dependent cyclic voltammograms of complex **1** in aqueous solution (Concentration: 0.03 mM, scan rate: 50 mV/s, Reference electrode: Ag/AgCl).

As Fig. 4 shown, a prominent catalytic wave at ca. pH = 10 appeared at 0.9 V for **1**, proving the complex was electrochemically active for driving water oxidation and potentially used for the modification of water oxidation electrodes.^{6a,b} In the range of pH 7-11, irreversible oxidation waves of **1** appeared between 0.8 and 1.0 V. At higher pH values (pH = 11), the lower potential wave at ca. 0.85 V grew in intensity and became the dominant for catalyzing water oxidation. The current of the complex **1** at higher pH values was stronger at lower pH values. According to the appearance of the voltammograms, we speculated that the catalysis would not occur only under kinetic conditions, as described by Savéant.²⁷

TOFs of Catalyzing Water Oxidation

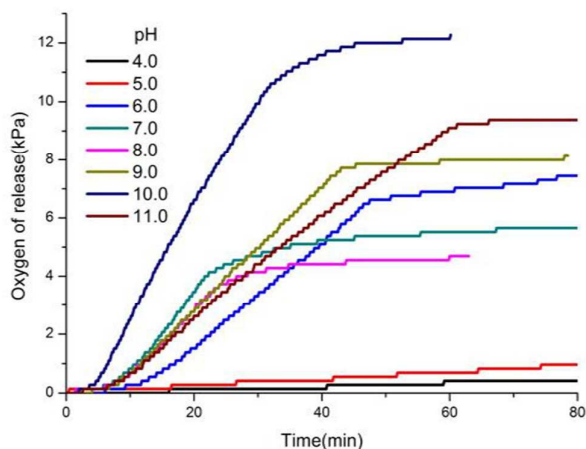


Fig. 5. The curves of releasing O₂ by water oxidation. Conditions: [PBS] = 0.1 M; [NaIO₄] = 0.036 M; [Macrocycle **1**] = 3.3 × 10⁻⁷ M.

The use of half-sandwich iridium in molecular catalysts for water oxidation originated with the work of Crabtree and co-workers.^{7,15} pentamethylcyclopentadienyl (Cp*) complexes as molecular precatalysts for water oxidation driven by cerium(IV) and NaIO₄ as sacrificial oxidants were reported by our group.^{6a,b} Herein, a

precursor of WOCs were described that bore the Cp* group along with a azo-compound ligand (Chart 1).

pH	Initial TOF (min ⁻¹) ^a
4.0	0.08
5.0	0.14
6.0	1.41
7.0	1.12
8.0	0.92
9.0	1.63
10.0	2.47
11.0	1.88

Table 1. Data of TOF. ([Cat] = 3.3 × 10⁻⁷ M; [PBS] = 0.1 M; NaIO₄ = 0.036 M; Volume of solution = 30 mL; Volume of oxygen is about 10 mL; T = 25 °C; solvent for the precatalyst = MeOH); ^a: according to PV = nRT, calculating TOF values.

The organometallic macrocycle **1** was isolated as water-soluble OTF salt, having four outer-sphere OTF ions. The macrocycle catalyzed water oxidation in the presence of NaIO₄ as sacrifice chemical oxidant in Fig. 5. The initial, maximal rate of oxygen evolution was affected by changes in pH values of solutions as Table 1 shown. The rate of oxygen evolution was greater in the solution of pH = 10 than in other solutions of various pH values. As Fig. 5 indicated, the (turnover frequency) TOFs reached up to 2.47 min⁻¹, slowly scrambled with higher pH values until the value arrived at 11.0. This value was less than around 10 min⁻¹ in the previous work,^{15d-g} however it had significance for a metallamacrocycle utilized as water-oxidation precatalyst. In order to confirm the evolving oxygen from the water-oxidation reaction, gas chromatography (GC) (GC-2014 Shimadzu; equipped with a thermal conductive detector, a 5 Å Molecular sieve column, and N₂ as carrier gas) was performed, unambiguously proving that the gas was oxygen as Figure 6 shown.

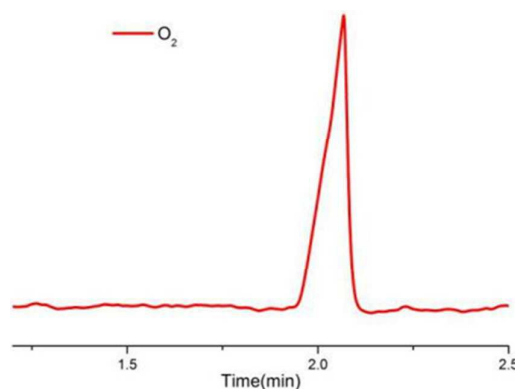
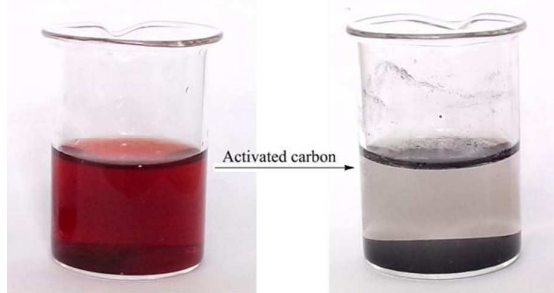
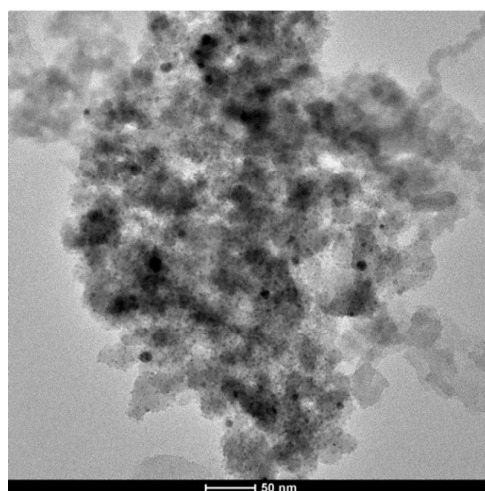


Fig. 6. GC spectrum of oxygen.

In order to tentatively overcome the major drawback of homogeneous catalysis, which is the need for separation and recovery from the reaction mixture at the end of the process, the facilitation of activated carbon is of importance to immobilize complex **1** into heterocatalyst, due to its a therm-steady porous material and favorably adsorbing dye compounds. The heterogeneous catalysis can be recyclable and readily separable from the reaction system, and offer the opportunity to reduce the impact on environment and increase industrial interest for the liquid phase oxidation catalytic process.²⁸ For this purpose, we employed activated carbon as catalysts loading materials for the heterogenization of the macrocycle **1**. When the activated carbon soaked in the macrocycle **1** solution for one day, the red solution became colorless (Fig. 7), preliminary indicating that the precatalyst was captured into the activated carbon. To further confirm the appoint, HRTEM (High Resolution Transmission Electron Microscopy) was carried out. As Fig. 8 shown, it clearly proved that **1** was thoroughly absorbed in the activated carbon.

Fig. 7. The images of **1** (left) and **1**/activated carbon (right).

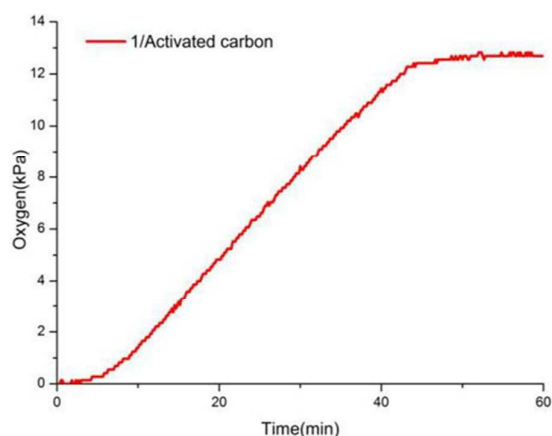
To further investigate TOF of **1**/activated carbon as heterocatalyst, it was employed taking part in water-oxidation reaction. In a typical experiment, **1**/activated carbon (2.0 mg), NaIO₄ (237.0 mg), PBS (pH = 10.0, 30.0 ml) were added in a sealed round bottom flask, and the reaction was performed under vigorous stirring at room temperature. The efficiency of the reaction in the system was monitored quantitatively by Transient Pressure Recorder (OM-CP-PRTRANS-1-30A) in Fig. 9 shown. As the figure exhibited, the TOF of the heterocatalysis was similar to those of the homocatalysis.

Fig. 8. The HRTEM image of **1**/activated carbon.

Supposed mechanism of the water oxidation reaction

Primitively, it indeed needed to explain why the TOF was the best in the solutions whose pH was near 9.0. In the light of previous work,⁶ OH⁻ radicals would attack the center of catalysts for water oxidation, resulting in forming a M-OH formula. Subsequently, this intermediate would be transformed into M=O, which was a key step for O₂-evolution. Therefore, the TOF of the precatalyst in basic solutions would be better.

According to previous work, the mechanism of WOCs based on half-sandwich iridium motifs, was that the formation of O-O bond was a key step in water oxidation, the Cp* and naphthol groups meanwhile was degraded into small molecules with NaIO₄.¹⁵ Therefore, we supposed the mechanism of metallamacrocycle **1** as catalysis for water-oxidation reaction was of a synchronous reaction. That is, when the precatalysis accomplished catalyzing water-oxidation reaction to evolve oxygen, the precatalysis was degraded into IrO_x.

Fig. 9. Oxygen of release via water oxidation catalyzed by **1**/activated carbon.

Conclusions

In conclusion, novel tetranuclear metallamacrocycles **1** and **2** based on half-sandwich fragments and a newly azo-compound are successfully constructed by coordination-orientation self-assembly. Due to this coordination orientation, supramolecular architectures of **1** and **2** are formed via H bonding between the azo-compound ligands and Cp* groups of half-sandwich fragments. In order to investigate electronic properties of the iridium-based compounds (complex **1**), cyclic voltammetry is performed, giving a result that the compound has a good potential of driving catalyze water-oxidation reaction. Hence the complex is explored as a precatalysis for water-oxidation reaction in the presence of NaIO₄ salt utilized as sacrificial chemical oxidant, offering a high TOFs which reaches up to 2.47 min⁻¹. Meanwhile, in order to investigate the behavior of its heterogeneous catalyst, the immobilization of complex **1** accesses immersion of activated carbon in its menthol solution for one day, giving **1/activated carbon** as heterocatalyst. When **1/activated carbon** takes part in water-oxidation reaction, gives a TOF similar to that of homocatalyst. Furthermore, Study of the mechanism of water-oxidation reaction promoted by such a metallacycle is currently underway.

Experimental Section

Experimental Details. All solvents were of commercial grade and dried over activated alumina using a Grubbs-type solvent purification system prior to use. ¹H, ¹³C and ¹⁹F NMR spectra were collected on a 400 MHz Bruker spectrometer. UV-vis spectra were collected using a Varian Cary 50 Bio UV-Vis spectrometer with samples in a 1.0 cm quartz cuvette at pH 7.0. The starting material [(Cp*)IrCl₂]₂ and [(Cp*)RhCl₂]₂ were prepared according to the literature methods.²⁹ Elemental analyses were performed on an Elementar III Vario El analyzer. IR spectra are measured on a Nicolet Avatar-360 spectrophotometer (as KBr pellet). Electrospray ionization mass spectra (ES-MS) were recorded on a Finnigan LCQ mass spectrometer using dichloromethane-methanol as mobile phase. Crystal samples of **1** and **2** used for X-ray crystallography were obtained by slow diffusion of ether into their methanol solutions.

Syntheses and Preparation

Ligand HL

To a magnetically stirred solution of 3-aminopyridine (2 mmol) and sodium nitrite (4 mL, 10%) in acetone (15 mL) was added supported one drop of dilute hydrochloric acid (10%). The reaction mixture was then stirred for one hour at room temperature, while stirring to obtain diazonium salt solution. The resulting diazonium salt was slowly added to the solution of 2-naphtol (2 mmol) in acetone and sodium hydroxide (10 mL, 5%) and was added to adjust the pH < 7.0, the reaction mixture was then stirred for 1 hour at room temperature. The solvent was evaporated at reduced pressure. The residue was precipitated, filtered and washed with diethyl ether to give the pure product. **Ligand:** Yield, 0.4g, 80%.

The ligand: ¹H NMR (400 MHz, CDCl₃, ppm): δ 6.882 (d, J = 9.6 Hz, 1H, naphthalene), 7.259 (s, 1H, naphthalene), 7.420 (m, 1H, naphthalene), 7.599 (m, 2H, naphthalene), 7.755(d, J = 9.2 Hz, 1H, naphthalene), 8.082 (d, J = 8.4 Hz, 1H, pyridine), 8.541 (m, 2H, pyridine), 8.961(s, 1H, pyridine), 15.891(s, 1H, hydroxyl). ¹³C NMR (100.6 MHz, CDCl₃, ppm): δ 121.881, 124.258, 124.428, 124.525, 126.271, 128.284, 128.797, 129.200, 130.918, 133.240, 140.890, 141.515, 148.065, 171.586.

[η⁵-Cp*Ir(L)]₄(OTf)₄ (**1**)

[Cp*IrCl₂]₂ (80.0 mg, 0.1mmol) were dissolved in 8.0 mL of methanol at room temperature. The solution was added into 4 equiv of AgOTf (103.0 mg, 0.4 mmol) and sheltered from light stirred vigorously over night. After then, the reaction solution was added to about 0.2 mmol (50.0 mg) of HL kept vigorously stirring for 6 hours, red precipitate collected by vacuum filtration in air. **1**, Yield, 64.3 mg, 65.0%.

Complex 1: ¹H NMR (400 MHz, d₆-DMSO, ppm): δ 1.674 (s, 15H, CH₃-Cp*), 7.286(d, J = 9.2 Hz, 1H, Ligand), 7.467 (m, 1H, Ligand), 7.726 (m, 1H, Ligand), 7.889(d, J = 8.0 Hz, 1H, Ligand), 8.281 (m, 1H, Ligand), 8.388 (d, J = 8.4 Hz, 1H, Ligand), 8.736 (d, J = 4.0 Hz, 1H, Ligand), 8.796 (d, J = 5.2 Hz, 1H, Ligand), 9.073 (d, J = 1.6 Hz, 1H, Ligand), 9.375 (s, 1H, Ligand). ¹³C NMR(100.6 MHz, d₆-DMSO, ppm): δ 8.960, 65.820, 95.673, 119.961, 123.163, 125.140, 125.636, 126.365, 126.501, 129.375, 129.861, 133.695, 135.264, 140.833, 147.446, 151.172, 153.217. ¹⁹F NMR(376.5 MHz, d₆-DMSO, ppm): δ -77.777. Elemental analysis calcd (%) for C₁₀₄H₁₀₀F₁₂Ir₄N₁₂O₁₆S₄: C, 43.09; H, 3.48; N, 5.80. Found: C, 43.02; H, 3.45; N, 5.68.

[η⁵-Cp*Rh(L)]₄(OTf)₄ (**2**)

[Cp*RhCl₂]₂ (61.0 mg, 0.1mmol) were dissolved in 8 mL of methanol at room temperature. The solution was added into 4 equiv of AgOTf (103.0 mg, 0.4 mmol) and sheltered from light stirred vigorously over night. After then, the reaction solution was added to about 0.2 mmol (50.0 mg) of HL kept vigorously stirring for 6 hours, red precipitate collected by vacuum filtration in air. **2**, Yield, 90.2 mg, 71.0%.

Complex 2: ¹H NMR (400 MHz, d₆-DMSO, ppm): δ 1.341 (s, 15H, CH₃-Cp*), 7.326(d, J = 8.8 Hz, 1H, Ligand), 7.425 (t, 1H, Ligand), 7.620 (t, 1H, Ligand), 7.738(b, 1H, Ligand), 7.840 (d, J = 7.6, 1H, Ligand), 8.111 (d, J = 9.2 Hz, 1H, Ligand), 8.370(d, J = 8.0 Hz, 1H, Ligand), 8.446 (d, J = 6.8 Hz, 1H, Ligand), 8.740 (s, 1H, Ligand), 9.135(s, 1H, Ligand). ¹³C NMR(100.6 MHz, d₆-DMSO, ppm): δ 9.062, 65.828, 98.952, 116.736, 119.966, 122.803, 123.170, 125.770, 126.327, 128.425, 129.483, 129.809, 134.442, 140.654, 146.527, 150.519, 152.937. ¹⁹F NMR(376.5 MHz, d₆-DMSO, ppm): δ -77.774. Elemental analysis calcd (%) for C₅₂H₅₀F₆N₆O₈Rh₂S₂: C, 49.14; H, 3.97; N, 6.61. Found: C, 49.08; H, 3.90; N, 6.58.

Preparation of 1/activated carbon

Activated carbon (100 mg) was soaked into the methanol solution of Macrocycle **1** (10 mg), and vigorously stirred for one day at

ambient temperature. When the solution became colorless, the black powder of **1/activated carbon** was obtained after filtration, and dried in air.

Catalyzing water-oxidation reaction in homogeneous/heterogeneous system

NaIO₄ (234.2 mg), precatalysis of the macrocycle **1/ 1/activated carbon** (8.0 mg/2.0 mg), and PBS (in the range of pH from 7.0 to 11.0, 30 ml) were added in a sealed round bottom flask, and the reaction was performed under vigorous stirring at room temperature. The efficiency of the reaction in the system was monitored quantitatively by Transient Pressure Recorder (OM-CP-PRTRANS-1-30A). In order to confirm the oxygen of release in water-oxidation reaction, GC was carried out.

X-ray crystal structure determinations

Data were collected on a CCD-Bruker SMART APEX system. All the determinations of unit cell and intensity data were performed with graphite-monochromated MoK α radiation ($\lambda = 0.71073 \text{ \AA}$). All the data were collected at room temperature using the ω scan technique. These structures were solved by direct methods, using Fourier techniques, and refined on F^2 by a full-matrix least-squares method. All the calculations were carried out with the SHELXTL program.³⁰ A summary of the crystallographic data and selected experimental information are given in supporting information.

Crystallographic data (excluding structure factors) for the structure analysis have been deposited with the Cambridge Crystallographic Data Centre, CCDC No. 1046417 (**1**) and No.1046418 (**2**). Copies of this information may be obtained free of charge on application to the Director, CCDC, 12 Union Road, Cambridge, CB21EZ, UK (fax: +44 1223 336033; e-mail: deposit@ccdc.cam.ac.uk or www: http://www.ccdc.cam.ac.uk).

Acknowledgements

This work was supported by the National Science Foundation of China (21301003, 21271006) and Anhui Provincial Science Foundation (1408085QB30).

Notes and references

1 (a) J.-M. Lehn, *Supramolecular Chemistry: Concepts and Perspectives*, VCH: Weinheim, Germany, 1995. (b) J. W. Steed and J. L. Atwood, *Supramolecular Chemistry*, John Wiley & Sons: West Sussex, U.K., 2000. (c) J. W. Steed, D. R. Turner and K. J. Wallace, *Core Concepts in Supramolecular Chemistry and Nanochemistry*, John Wiley & Sons: West Sussex, U.K., 2007. (d) M. M. Conn and J., Jr. Rebek, *Chem. Rev.* 1997, **97**, 1647-1668. (e) D. Ajami and J., Jr. Rebek, *Acc. Chem. Res.* 2013, **46**, 990. (f) F. M. Raymo and J. F. Stoddart, *Chem. Rev.* 1999, **99**, 1643. (g) R. S. Forgan, J.-P. Sauvage and J. F. Stoddart, *Chem. Rev.* 2011, **111**, 5434. (h) L. Brunsveld, B. J. B. Folmer, E. W. Meijer and R. P. Sijbesma, *Chem. Rev.* 2001, **101**, 4071.

2 (a) M. Fujita, M. Tominaga, A. Hori and B. Therrien, *Acc. Chem. Res.* 2005, **38**, 369. (b) M. D. Pluth and K. N. Raymond, *Chem. Soc. Rev.* 2007, **36**, 161. (c) S. Liu, Y.-F. Han and G.-X. Jin, *Chem. Soc. Rev.* 2007, **36**, 1543. (d) C. G. Oliveri, P. A. Ulmann, M. J. Wiester and C. A. Mirkin, *Acc. Chem. Res.* 2008, **41**, 1618. (e) G. R. Newkome and C. Shreiner, *Chem. Rev.* 2010, **110**, 6338. (f) P. J. Stang and B. Olenyuk, *Acc. Chem. Res.* 1997, **30**, 502. (g) S. R. Seidel and P. J. Stang, *Acc. Chem. Res.* 2002, **35**, 972. (h) S. Leininger, B. Olenyuk and P. J. Stang, *Chem. Rev.* 2000, **100**, 853. (i) Y. Takezawa and M. Shionoya, *Acc. Chem. Res.* 2012, **45**, 2066. (j) M. Yoshizawa and J. K. Klosterman, *Chem. Soc. Rev.* 2014, **43**, 1885.

3 (a) M. Yoshizawa, M. Tamura and M. Fujita, *Science* 2006, **312**, 251. (b) M. Yoshizawa, M. Tamura and M. Fujita, *Angew. Chem., Int. Ed.* 2007, **46**, 3874. (c) K. Harano, S. Hiraoka and M. Shionoya, *J. Am. Chem. Soc.* 2007, **129**, 5300. (d) G. H. Clever, S. Tashiro and M. Shionoya, *J. Am. Chem. Soc.* 2010, **132**, 9973. (e) S. Freye, J. Hey, A. Torras-Galan, D. Stalke, R. Herbst-Irmer, M. John and G. H. Clever, *Angew. Chem., Int. Ed.* 2012, **51**, 2191. (f) S. Freye, R. Michel, D. Stalke, M. Pawliczek, H. Frauendorf and G. H. Clever, *J. Am. Chem. Soc.* 2013, **135**, 8476. (g) N. Kishi, Z. Li, K. Yoza, M. Akita and M. Yoshizawa, *J. Am. Chem. Soc.* 2011, **133**, 11438.

4 (a) M. Fujita, J. Yazaki and K. Ogura, *J. Am. Chem. Soc.* 1990, **112**, 5647. (b) P. J. Stang and D. H. Cao, *J. Am. Chem. Soc.* 1994, **116**, 4981. (c) Y. K. Kryschenko, S. R. Seidel, A. M. Arif and P. J. Stang, *J. Am. Chem. Soc.* 2003, **125**, 5193. (d) H.-B. Yang, N. Das, F. Huang, A. M. Hawkridge, D. C. Muddiman and P. J. Stang, *J. Am. Chem. Soc.* 2006, **128**, 10014. (e) H.-B. Yang, K. Ghosh, Y. Zhao, B. H. Northrop, M. M. Lyndon, D. C. Muddiman, H. S. White and P. J. Stang, *J. Am. Chem. Soc.* 2008, **130**, 839. (f) L. Zhao, B. H. Northrop and P. J. Stang, *J. Am. Chem. Soc.* 2008, **130**, 11886. (g) C. G. Oliveri, N. C. Gianneschi, S. T. Nguyen, C. A. Mirkin, C. L. Stern, Z. Wawrzak and M. Pink, *J. Am. Chem. Soc.* 2006, **128**, 16286. (h) H. J. Yoon, J. Heo and C. A. Mirkin, *J. Am. Chem. Soc.* 2007, **129**, 14182. (i) N. Kishi, M. Akita, M. Kamiya, S. Hayashi, H.-F. Hsu and M. Yoshizawa, *J. Am. Chem. Soc.* 2013, **135**, 12976.

5 Z.-Y. Li, Y. Zhang, C.-W. Zhang, L.-J. Chen, C. Wang, H. Tan, Y. Yu, X. Li and H.-B. Yang, *J. Am. Chem. Soc.* 2014, **136**, 8577.

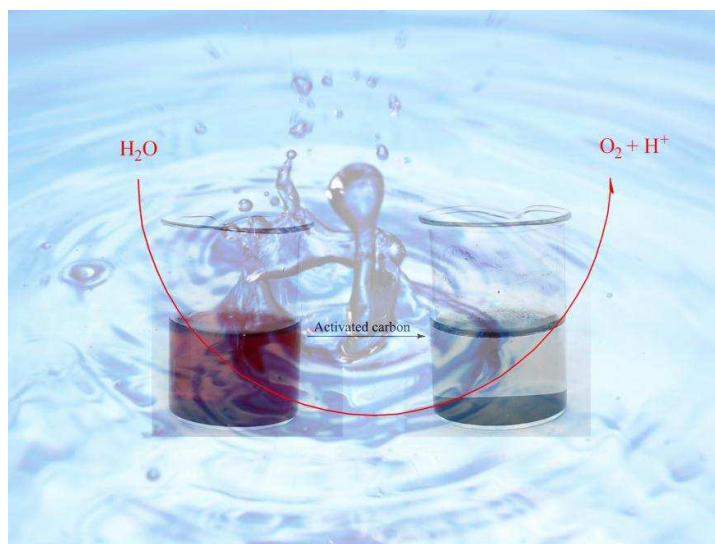
6 (a) W. -B. Yu, Q. -Y. He, H. -T. Shi, J. -Y. Jia and X. Wei, *Dalton Trans.* 2014, **43**, 6561. (b) W. -B. Yu, Q. -Y. He, H. -T. Shi, Y. Pan and X. Wei, *Dalton Trans.* 2014, **43**, 12221. (c) W. -B. Yu, Q. -Y. He, H. -T. Shi, G. Yuan and X. Wei, *Chem. Asian J.* 2015, **10**, 239. (d) Y.-F. Han, L. Zhang, L.-H. Weng and G.-X. Jin, *J. Am. Chem. Soc.*, 2014, **136**, 14608. (e) Y.-F. Han and G.-X. Jin, *Chem. Soc. Rev.*, 2014, **43**, 2799. (f) H. Li, Y.-F. Han and G.-X. Jin, *J. Am. Chem. Soc.*, 2014, **136**, 2982. (g) Y.-F. Han, G.-X. Jin, and F. E. Hahn, *J. Am. Chem. Soc.*, 2013, **135**, 9263. (h) Y.-F. Han, H. Li, L.-H. Weng and G.-X. Jin, *Chem. Commun.*, 2010, 3556. (i) L. Zhang, Y.-J. Lin, Z.-H. Li and G.-X. Jin, *J. Am. Chem. Soc.* 2015, **137**, 13670. (j) X.-Y. Shen, Y.-Y. Zhang, L. Zhang, Y.-J. Lin and G.-X. Jin, *Chem.-Eur. J.* 2015, **21**, 16975. (k) Y.-Y. Zhang, L. Zhang, Y.-J. Lin and G.-X. Jin, *Chem.-Eur. J.* 2015, **21**, 14893-14900.

- 7 (a) J. D. Blakemore, N. D. Schley, D. Balcells, J. F. Hull, G. W. Olack, C. D. Incarvito, O. Eisenstein, G. W. Brudvig and R. H. Crabtree, *J. Am. Chem. Soc.* 2010, **132**, 16017. (b) U. Hintermair, J. Campos, T. P. Brewster, L. M. Pratt, N. D. Schley and R. H. Crabtree, *ACS Catal.* 2014, **4**, 99. (c) J. M. Thomsen, S. W. Sheehan, S. M. Hashmi, J. Campos, U. Hintermair, R. H. Crabtree and G. W. Brudvig, *J. Am. Chem. Soc.*, 2014, **136**, 13826. (d) J. D. Blakemore, R. H. Crabtree and G. W. Brudvig, 2015, DOI: 10.1021/acs.chemrev.5b00122. (e) D. Y. Shopov, B. Rudsteyn, J. Campos, V. S. Batista, R. H. Crabtree and G. W. Brudvig, *J. Am. Chem. Soc.*, 2015, **137**, 7243. (f) J. Graeupner, U. Hintermair, D. L. Huang, J. M. Thomsen, M. Takase, J. Campos, S. M. Hashmi, M. Elimelech, G. W. Brudvig and R. H. Crabtree, *Organometallics*, 2013, **32**, 5384. (g) U. Hintermair, S. W. Sheehan, A. R. Parent, D. H. Ess, D. T. Richens, P. H. Vaccaro, G. W. Brudvig and R. H. Crabtree, *J. Am. Chem. Soc.*, 2013, **135**, 10837. (h) J. D. Blakemore, M. W. Mara, M. N. Kushner-Lenhoff, N. D. Schley, S. J. Konezny, I. Rivalta, C. F. A. Negre, R. C. Snoeberger, O. Kokhan, J. Huang, A. Stickrath, L. A. Tran, M. L. Parr, L. X. Chen, D. M. Tiede, V. S. Batista, R. H. Crabtree and G. W. Brudvig, *Inorg. Chem.*, 2013, **52**, 1860.
- 8 R. Lalrempuia, N. D. McDaniel, H. Müller-Bunz, S. Bernhard and M. Albrecht, *Angew. Chem., Int. Ed.* 2010, **49**, 9765.
- 9 A. Savini, G. Bellachioma, G. Ciancaleoni, C. Zuccaccia, D. Zuccaccia and A. Macchioni, *Chem. Commun.* 2010, **46**, 9218.
- 10 D. G. H. Hettterscheid and J. N. H. Reek, *Chem. Commun.* 2011, **47**, 2712.
- 11 D. B. Grotjahn, D. B. Brown, J. K. Martin, D. C. Marelus, M.-C. Abadjian, H. N. Tran, G. Kalyuzhny, K. S. Vecchio, Z. G. Specht, S. A. Cortes-Llamas, V. Miranda-Soto, C. van Niekerk, C. E. Moore and A. L. Rheingold, *J. Am. Chem. Soc.* 2011, **133**, 19024.
- 12 D. Hong, M. Murakami, Y. Yamada and S. Fukuzumi, *Energy Environ. Sci.* 2012, **5**, 5708.
- 13 A. Bucci, A. Savini, L. Rocchigiani, C. Zuccaccia, S. Rizzato, A. Albinati, A. Llobet and A. Macchioni, *Organometallics* 2012, **31**, 8071.
- 14 Z. Codola, M. S. J. Cardoso, B. Royo, M. Costas and J. Lloret-Fillol, *Chem.-Eur. J.* 2013, **19**, 7203.
- 15 (a) J. F. Hull, D. Balcells, J. D. Blakemore, C. D. Incarvito, O. Eisenstein, G. W. Brudvig and R. H. Crabtree, *J. Am. Chem. Soc.* 2009, **131**, 8730. (b) U. Hintermair, S. W. Sheehan, A. R. Parent, D. H. Ess, D. T. Richens, P. H. Vaccaro, G. W. Brudvig and R. H. Crabtree, *J. Am. Chem. Soc.* 2013, **135**, 10837. (c) J. M. Thomsen, S. W. Sheehan, S. M. Hashmi, J. Campos, U. Hintermair, R. H. Crabtree and G. W. Brudvig, *J. Am. Chem. Soc.*, 2014, **136**, 13826. (d) M. Zhou, N. D. Schley and R. H. Crabtree, *J. Am. Chem. Soc.* 2010, **132**, 12550. (e) M. Zhou, D. Balcells, A. R. Parent, R. H. Crabtree and O. Eisenstein, *ACS Catal.* 2012, **2**, 208. (f) J. D. Blakemore, N. D. Schley, D. Balcells, J. F. Hull, G. W. Olack, C. D. Incarvito, O. Eisenstein, G. W. Brudvig and R. H. Crabtree, *J. Am. Chem. Soc.* 2010, **132**, 16017. (g) A. Savini, G. Bellachioma, G. Ciancaleoni, C. Zuccaccia, D. Zuccaccia, A. Macchioni, *Chem. Commun.* 2010, **46**, 9218.
- 16 J. O. M. Bockris, *Energy: The Solar-Hydrogen Alternative*, 1st ed.; Halsted Press: New York, 1975.
- 17 M. Gratzel, *Acc. Chem. Res.* 1981, **14**, 376.
- 18 T. J. Meyer, *Acc. Chem. Res.* 1989, **22**, 163.
- 19 N. S. Lewis, and D. G. Nocera, *Proc. Natl. Acad. Sci. U.S.A.* 2006, **103**, 15729.
- 20 D. Gust, T. A. Moore, and A. L. Moore, *Acc. Chem. Res.* 2009, **42**, 1890.
- 21 M. G. Walter, E. L. Warren, J. R. McKone, S. W. Boettcher, Q. Mi, E. A. Santori and N. S. Lewis, *Chem. Rev.* 2010, **110**, 6446.
- 22 R. H. Crabtree, *Energy Production and Storage-Inorganic Chemistry Strategies for a Warming World*; John Wiley & Sons: Hoboken, 2010.
- 23 K. J. Young, L. A. Martini, R. L. Milot, R. C. Snoeberger, V. S. Batista, C. A. Schmuttenmaer, R. H. Crabtree and G. W. Brudvig, *Coord. Chem. Rev.* 2012, **256**, 2503.
- 24 H. Dau, C. Limberg, T. Reier, M. Risch, S. Roggan and P. Strasser, *ChemCatChem* 2010, **2**, 724.
- 25 (a) R. Chakrabarty, P. S. Mukherjee and P. J. Stang, *Chem. Rev.* 2011, **111**, 6810. (b) T. R. Cook, Y.-R. Zheng and P. J. Stang, *Chem. Rev.* 2013, **113**, 734. (c) T. R. Cook and P. J. Stang, *Chem. Rev.* 2015, **115**, 7001.
- 26 M. Mirjalili, F. Zahed and A. Hassanabadi, *E-J. Chem.*, 2012, **9**, 1042.
- 27 J.-M. Savéant, *Chem. Rev.* 2008, **108**, 2348.
- 28 L. Ma, F. Su, W. Guo, S. Zhang, Y. Guo and J. Hu, *Microporous Mesoporous Mater.* 2013, **169**, 16.
- 29 C. White, A. Yates and P. M. Maitlis, *Inorg. Synth.* 1992, **29**, 228.
- 30 G. M. Sheldrick, *Shelxl-97*; Universität Göttingen: Germany, 1997.

Table of Contents

Homo-/Heterogeneous Catalysis of Water Oxidation Supported by a Newly Metallamacrocyclic

Wei-Bin Yu*, Qing-Ya He, Hua-Tian Shi, and Xianwen Wei



Metallamacrocycles **1** and **2** were constructed, and **1** was further explored as precatalyst for water oxidation, giving a good efficiency.